Available online at www.sciencedirect.com
ScienceDirect
Journal of Sound and Vibration 315 (2008) 732–745
JOURNAL OF SOUND AND VIBRATION
www.elsevier.com/locate/jsvi

Targeted energy transfer in systems with non-polynomial nonlinearity

Oleg V. Gendelman*

Faculty of Mechanical Engineering, Technion—Israel Institute of Technology, Technion City, Haifa 32000, Israel

Accepted 13 December 2007
The peer review of this article was organised by the Guest Editor
Available online 30 January 2008

Abstract

Targeted energy transfer (TET) in a 2dof system consisting of primary linear oscillator and nonlinear energy sink (NES) with non-polynomial potential is investigated. Use of non-polynomial and even non-analytic potential functions is motivated by needs of practical design. It is demonstrated that the "complexification–averaging" technique of analysis developed before can be successfully extended for these cases with proper modifications. The procedure is illustrated by examples involving softening (non-polynomial) and piecewise-linear (non-analytic) NES.

1. Introduction

Targeted energy transfer (TET), i.e. almost irreversible passive transfer of mechanical energy from linear substructure to essentially nonlinear attachment (nonlinear energy sink (NES)) has attracted a lot of attention of researches in the few last years [1–6]. In majority of these models, stiff nonlinear attachments (commonly, purely cubic spring) were used. In accordance, the methods of analysis were crafted for systems with cubic (or, in general, polynomial [3]) nonlinearity and linear damping.

Still, in the same time, it was demonstrated that some designs of the NES may be rather advantageous for the TET and do not fall into the class of the polynomial nonlinearities. For instance, it was demonstrated [7] that the NES with a piecewise-linear potential can exhibit profound TET. Besides, in many applications—especially those where geometric nonlinearity is involved—the nonlinear springs are soft.

The main goal of this paper is to extend existing methods for analysis of the TET in 2dof systems for the case of the NES with non-polynomial potentials. In Section 2, the general framework of the analysis is considered. In Sections 3 and 4, the methodology outlined is tested for two benchmark problems—NES with a soft nonlinearity and a piecewise linear NES.

*Tel.: +972 4 8293877; fax: +972 4 8295711.
E-mail address: ovgend@tx.technion.ac.il

0022-460X/$ - see front matter
doi:10.1016/j.jsv.2007.12.024

2. Description of the model and general analysis

Let us consider the following system [3], which consists of linear oscillator and small strongly nonlinear attachment and is described by the set of equations:

$$\begin{aligned} &\ddot{y}_1 + \varepsilon\lambda(\dot{y}_1 - \dot{y}_2) + y_1 + \varepsilon F(y_1 - y_2) = 0, \\ &\varepsilon\ddot{y}_2 + \varepsilon\lambda(\dot{y}_2 - \dot{y}_1) + \varepsilon F(y_2 - y_1) = 0, \end{aligned} \tag{1}$$

where $\varepsilon \ll 1$ is a small parameter which establishes the order of magnitude for coupling, damping and mass of the nonlinear attachment, λ is a damping coefficient. If there exists a small (of order ε) damping on the primary oscillator, it also may be taken into account; in current treatment it does not change the situation qualitatively and is omitted for the sake of brevity. The coupling terms are considered to be symmetric and therefore the function $F(x)$ is adopted to be odd:

$$F(x) = -\frac{\partial V(x)}{\partial x} = -F(-x). \tag{2}$$

Mass of the attachment is considered to be small related to the mass of the main oscillator. Stiffness and damping of the attachment are adopted to depend only on relative displacement of the attachment and the main mass. Both these conditions have obvious motivation from the viewpoint of possible applications: NES is designed to have small mass compared with the main system and does not need alternative grounding.

The treatment follows general framework developed in paper [3], but with some essential modifications. Change of variables

$$v = y_1 + \varepsilon y_2, \quad w = y_1 - y_2 \tag{3}$$

physically corresponds to transition to "center of mass—relative displacement" coordinates and allows reducing Eq. (1) to the following form:

$$\begin{aligned} &\ddot{v} + \frac{v + \varepsilon w}{(1+\varepsilon)} = 0, \\ &\ddot{w} + \frac{v + \varepsilon w}{1+\varepsilon} + (1+\varepsilon)\lambda\dot{w} + (1+\varepsilon)F(w) = 0. \end{aligned} \tag{4}$$

It should be mentioned that the damping terms have disappeared from the first equation of Eq. (4) due to supposed gradient character of the damping.

The goal of present investigation is the exploration of damped nonlinear normal modes of Eq. (1) in the vicinity of 1:1 resonance. It means that both variables, v and w, are supposed to have frequency close to unity.

Complex variables [8] are introduced according to following relationship:

$$\begin{aligned} &\varphi_1 \exp(\mathrm{i}t) = \dot{v} + \mathrm{i}v, \\ &\varphi_2 \exp(\mathrm{i}t) = \dot{w} + \mathrm{i}w. \end{aligned} \tag{5}$$

As it is demonstrated in Ref. [3], if the dynamical flow is considered in the vicinity of 1:1 resonance manifold, then functions φ_1 and φ_2 may be considered as functions of slow time scale. Formal applicability of such procedure for essentially nonlinear system beyond the conditions of the averaging theory is discussed in Ref. [9].

Formal averaging of Eq. (4) with account of anzats (5) with respect to the fast time scale is possible if the function $F(w)$ is presented in a form of Fourier series:

$$F(w) = F\left(-\frac{\mathrm{i}}{2}(\varphi_2 \exp(\mathrm{i}t) - \varphi_2^* \exp(-\mathrm{i}t)\right) = \sum_{j=-\infty}^{\infty} f_j(\varphi_2, \varphi_2^*)\exp(\mathrm{i}jt). \tag{6}$$

Averaged Eq. (4) will take the form

$$\begin{aligned}&\dot{\varphi}_1+\frac{\mathrm{i}\varepsilon}{2(1+\varepsilon)}(\varphi_1-\varphi_2)=0,\\&\dot{\varphi}_2+\frac{\mathrm{i}}{2(1+\varepsilon)}(\varphi_2-\varphi_1)+\frac{\lambda(1+\varepsilon)}{2}\varphi_2+(1+\varepsilon)f_1(\varphi_2,\varphi_2^*)=0,\end{aligned}\tag{7}$$

where f_1 is the first Fourier coefficient:

$$f_1=\frac{1}{2\pi}\int_0^{2\pi}F\left(-\frac{\mathrm{i}}{2}\left(\varphi_2\exp(\mathrm{i}t)-\varphi_2^*\exp(-\mathrm{i}t)\right)\right)\exp(-\mathrm{i}t)\,\mathrm{d}t.\tag{8}$$

The integral may be computed, for instance, with the help of residues. In order to establish the general shape of function f_1 one can adopt than in some vicinity of zero the function $F(w)$ is analytic and may be presented as Taylor series:

$$F(w)=\sum_{j=0}^{\infty}a_j w^{2j+1}.\tag{9}$$

Shape of series (9) takes into account the oddity of function F. With account of Eqs. (5) and (6), by using binomial expansion for each term in Eq. (9) and collecting the coefficients of $\exp(\mathrm{i}t)$, one obtains

$$\begin{aligned}f_1(\varphi_2,\varphi_2^*)&=-\frac{\mathrm{i}\varphi_2}{2}\sum_{k=0}^{\infty}(-1/4)^k a_k C_{2k+1}^{k+1}|\varphi_2|^{2k}=-\frac{\mathrm{i}\varphi_2}{2}G\left(|\varphi_2|^2\right)\\C_{2k+1}^{k+1}&=\frac{(2k+1)!}{k!(k+1)!}.\end{aligned}\tag{10}$$

It is easy to see that if series (9) converges in some vicinity of zero, then series (10) also converges in some vicinity of zero and therefore real analytic function $G(z)$ is defined in this vicinity. If series (9) ceases to converge (it will be demonstrated below, that such situation may be of essential interest), one can still use analytic continuation of function G; obviously, the shape of function f_1 will remain the same. Finally, the averaged equations may be written in a form

$$\begin{aligned}&\dot{\varphi}_1+\frac{\mathrm{i}\varepsilon}{2(1+\varepsilon)}(\varphi_1-\varphi_2)=0,\\&\dot{\varphi}_2+\frac{\mathrm{i}}{2(1+\varepsilon)}(\varphi_2-\varphi_1)+\frac{\lambda(1+\varepsilon)}{2}\varphi_2-\frac{\mathrm{i}(1+\varepsilon)\varphi_2}{2}G\left(|\varphi_2|^2\right)=0.\end{aligned}\tag{11}$$

System of Eq. (11), generally speaking, is not solvable and further simplifications are necessary. It should be mentioned that system (11) is integrable for $\lambda=0$, but we are interested in the damped case $\lambda>0$ (in fact, we suggest that $\lambda\gg\varepsilon$ and therefore λ is considered to be of order unity in the framework of current treatment). System (11) may be analyzed by multiple scales approach:

$$\frac{\mathrm{d}}{\mathrm{d}t}=\frac{\partial}{\partial\tau_0}+\varepsilon\frac{\partial}{\partial\tau_1}+\cdots.\tag{12}$$

For order $O(1)$ expansion (12) yields

$$\begin{aligned}&\frac{\partial\varphi_1}{\partial\tau_0}=0\Rightarrow\varphi_1=\varphi_1(\tau_1),\\&\frac{\partial\varphi_2}{\partial\tau_0}+\frac{\mathrm{i}}{2}\varphi_2+\frac{\lambda}{2}\varphi_2-\frac{\mathrm{i}\varphi_2}{2}G\left(|\varphi_2|^2\right)=\frac{\mathrm{i}}{2}\varphi_1.\end{aligned}\tag{13}$$

Fixed points $\Phi(\tau_1)$ of Eq. (13) are computed as

$$\frac{i}{2}\Phi+\frac{\lambda}{2}\Phi-\frac{\mathrm{i}}{2}G\left(|\Phi|^2\right)\Phi=\frac{\mathrm{i}}{2}\varphi_1(\tau_1).\tag{14}$$

Quite obviously, $\Phi(\tau_1) = \lim_{\tau_0 \to +\infty} \varphi_2(\tau_0, \tau_1)$ if this fixed point is stable and $\Phi(\tau_1) = \lim_{\tau_0 \to -\infty} \varphi_2(\tau_0, \tau_1)$ if the fixed point is unstable. It is easy to demonstrate that Eq. (13) does not have any limit sets besides the fixed points (for instance, with the help of Bendixson criterion—see details in Appendix A).

Solution of Eq. (14) requires knowledge of the coefficient λ and function G. Let us consider some stable (with respect to time scale τ_0) solution $\Phi(\tau_1)$. At time scale $O(\varepsilon)$ the first equation of system (11) taken in the limit $\tau_0 \to \infty$ yields

$$\frac{\partial \varphi_1}{\partial \tau_1} + \frac{\mathrm{i}}{2}(\varphi_1 - \Phi) = 0.$$

By substituting Eq. (14) to this expression, one obtains equation for Φ with respect to the slow time scale:

$$\frac{\partial}{\partial \tau_1}\left(\Phi - \mathrm{i}\lambda\Phi - \Phi G\left(|\Phi|^2\right)\right) + \frac{\lambda}{2}\Phi - \frac{\mathrm{i}}{2}\Phi G\left(|\Phi|^2\right) = 0. \tag{15}$$

By splitting to modulus and argument parts

$$\Phi = N(\tau_1)\exp(\mathrm{i}\delta(\tau_1)),$$

one finally obtains

$$\begin{aligned}\frac{\partial N}{\partial \tau_1} &= \frac{-\lambda N}{2(1+\lambda^2+G^2(N^2)-2G(N^2)-2N^2G'(N^2)+2N^2G(N^2)G'(N^2))},\\ \frac{\partial \delta}{\partial \tau_1} &= \frac{-\lambda^2+G(N^2)-G^2(N^2)-2N^2G(N^2)G'(N^2)}{2(1+\lambda^2+G^2(N^2)-2G(N^2)-2N^2G'(N^2)+2N^2G(N^2)G'(N^2))}.\end{aligned} \tag{16}$$

Quite surprisingly, system (16) is completely integrable regardless the shape of function $G(z)$. The first equation may be trivially reduced to quadrature and the solution of the second one requires one more integration if the first one is already solved. Of course, technically such computations may be extremely cumbersome, especially for complicated shapes of $G(z)$ but the qualitative behavior of the solutions will remain relatively simple due to this integrability.

The approximation of the fast time (13) will describe the response of the system to initial conditions, when the system approaches the resonance manifold, and Eq. (16) describes the slow-time evolution of the system at the manifold. Eq. (13) is, generally speaking, non-integrable, but still it has only two-dimensional state space and therefore the behavior of the solutions may be conveniently analyzed. Thus, the approximation developed above allows description of both initial-period asymptotics (boundary layer) and slow-time asymptotics (main solution). In the next sections, the methodology is applied for analysis of two different types of the nonlinear attachments.

3. NES with softening nonlinearity

In many applications, the nonlinearity is soft and cannot be described by simple polynomial potential function. For the sake of modelling, the potential of the attachment is chosen in the form

$$V(x) = k\,\ln(1 + x^2) \tag{17}$$

providing linear limit with stiffness coefficient $2\varepsilon k$ in Eq. (1) for small deformations z and softening while z grows. The shape of the potential function (17) is presented at Fig. 1.

Equations describing the system dynamics are

$$\begin{aligned}&\ddot{y}_1 + y_1 + \varepsilon\lambda(\dot{y}_1 - \dot{y}_2) + \frac{2\varepsilon k(y_1 - y_2)}{1 + (y_1 - y_2)^2} = 0,\\ &\varepsilon\ddot{y}_2 + \varepsilon\lambda(\dot{y}_2 - \dot{y}_1) + \frac{2\varepsilon k(y_2 - y_1)}{1 + (y_1 - y_2)^2} = 0,\end{aligned} \tag{18}$$

where y_1 and y_2 are the displacements of the primary oscillator and the attachment, respectively.

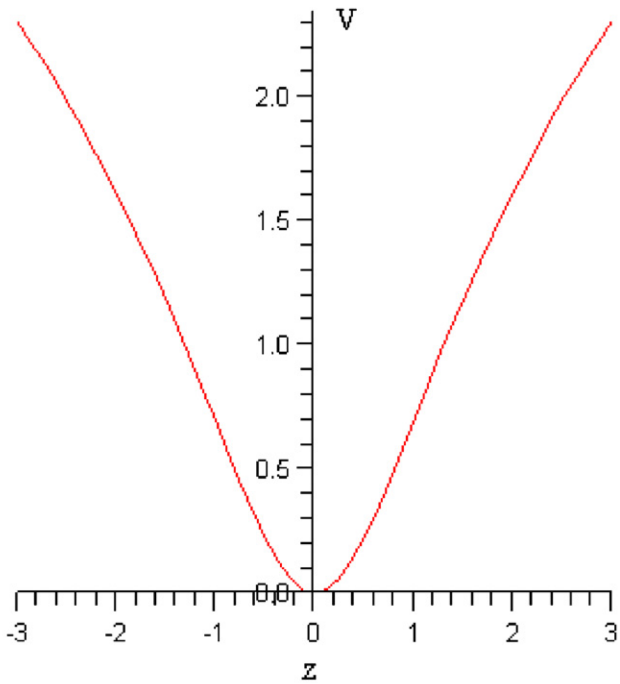

Fig. 1. The shape of potential function (17)—soft nonlinearity without possibility of breakdown, $k = 1$.

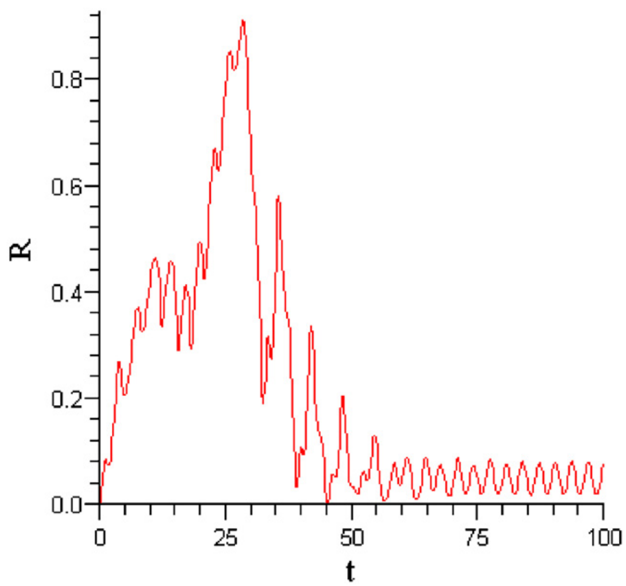

Fig. 2. Relative instantaneous energy in the attachment, $A = 1.3$.

3.1. TET—numeric demonstration

The phenomenon of the TET may be demonstrated numerically if system (18) is modelled with initial conditions $y_1(0) = 0,\ \dot{y}_1(0) = A,\ y_2(0) = 0,\ \dot{y}_2(0) = 0$. In order to demonstrate the targeted transfer, we plot the relative instantaneous energy $R = E_{att}/(E_{primary} + E_{att})$ stored in the attachment with respect to total

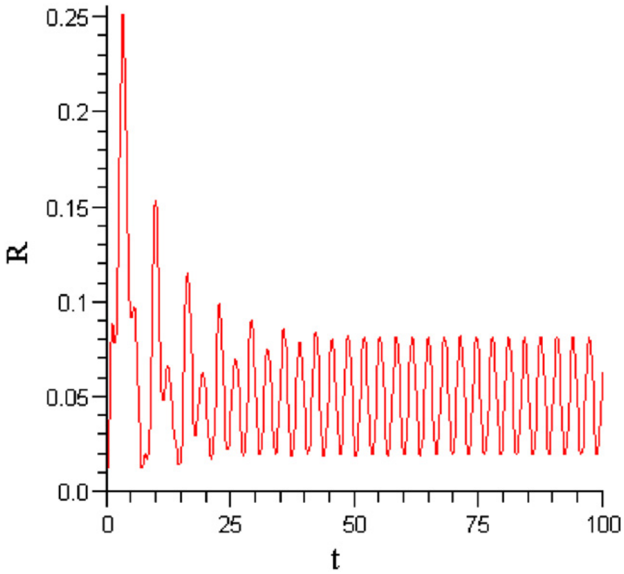

Fig. 3. Relative instantaneous energy in the attachment, $A = 0.8$.

energy of the system, where

$$E_{\text{primary}} = \tfrac{1}{2}\left(\dot{y}_1^2 + y_1^2\right),$$
$$E_{\text{att}} = \varepsilon\left(\tfrac{1}{2}\dot{y}_2^2 + k\,\ln(1 + (y_1 - y_2)^2)\right) \tag{19}$$

for two different values of initial velocity A and parameters of the system $\varepsilon = 0.05$, $k = 2$, $\lambda = 0.2$ (Figs. 2 and 3):

It is clear that for sufficient initial excitation the system exhibits vigorous targeted transfer of energy to the light attachment (for $t \sim 30$ about 90% of the total energy is concentrated at the attachment, whereas the linear characteristic time of the system is $1/\varepsilon\lambda = 100$). The mechanism of the energy transfer is resonance capture, which occurs due to soft nonlinearity. At small deformations, the linear frequency of the attachment is $\omega_0 = \sqrt{2k\varepsilon/\varepsilon} = 2$. Due to softening, when the deformations are large enough, the attachment can achieve 1:1 resonance with primary oscillator in the vicinity of unit frequency. Then, due to damping, the system is taken out from the resonance and energy remains at the attachment.

As it was already mentioned above, analytic description of the process of targeted transfer has been performed by combined method of complexification and averaging [8]. This method works directly only for polynomial-type nonlinearities, which is not the case in the problem under consideration. For Eq. (18), one may be tempted to use similar method, by presenting the nonlinear potential of the attachment as Taylor series with respect to $y_1 - y_2$ and keeping few first terms. Such approach is not valid if one is interested in the regime where displacements can be comparatively large (of course, it is the case for the problem of the targeted transfer) since the Taylor series will converge only for $|y_1 - y_2| < 1$. In order to circumvent this obstacle, we are going to use the method of Fourier-series expansion presented in Section 3. After averaging and computing the Fourier coefficient in accordance with (10, 11) one gets the following slow-flow equations:

$$\dot{\varphi}_1 + \frac{i\varepsilon}{2(1+\varepsilon)}(\varphi_1 - \varphi_2) = 0,$$
$$\dot{\varphi}_2 + \frac{i}{2(1+\varepsilon)}(\varphi_2 - \varphi_1) + \frac{\lambda(1+\varepsilon)}{2}\varphi_2 - \frac{i(1+\varepsilon)}{2}G\left(|\varphi_2|^2\right)\varphi_2 = 0,$$
$$G(z) = \frac{4k}{z}\left(1 - \frac{1}{\sqrt{1+z}}\right). \tag{20}$$

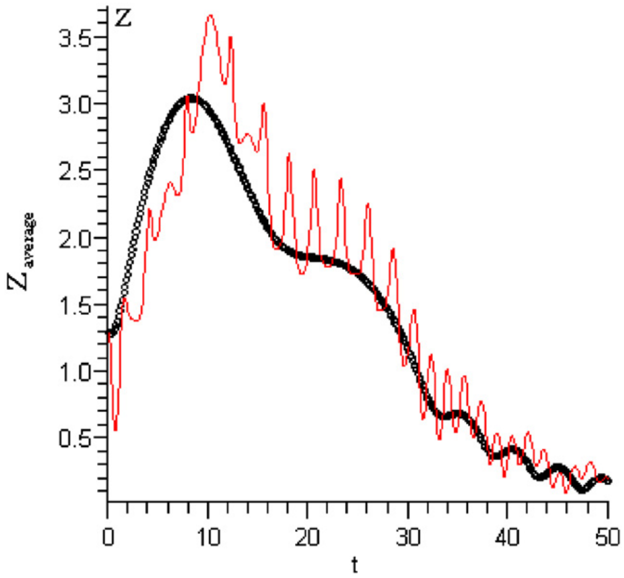

Fig. 4. Comparison between initial flow (solid line) and averaged flow (dotted line). $A = 1.3$.

Function $G(z)$ is computed from the expression for potential (17), with account of Eqs. (2), (5) and (8). Details of computation are presented in Appendix B.

Validity of the averaging procedure for description of the targeted transfer is illustrated at Fig. 4 by direct comparison between simulated flows of systems (18) and (20) with appropriate corresponding initial conditions, computed with the help of anzats (2). We compare the values $Z = \sqrt{(y_1(t) - y_2(t))^2 + (\dot{y}_1(t) - \dot{y}_2(t))^2}$ (solid line) and $Z_{\text{average}} = |\varphi_2|$ (dotted line).

The averaged flow, as expected, does not reflect the fast oscillations of the transient response, but clearly predicts the characteristic shape of the response curve, at least at important initial stages of the process (time scale of order $O(1/\varepsilon)$). Therefore, despite non-polynomial nonlinear function, the approach based on Fourier-series expansion (which may be treated as enhanced harmonic balance with respect to the fast time scale) yields rather reliable results.

3.2. Asymptotic analysis—order O(1)

Asymptotic analysis at order $O(1)$ is performed with the help of Eq. (13) with function $G(z)$ defined by Eq. (20):

$$\begin{aligned}
&\frac{\partial \varphi_2}{\partial \tau_0} + \frac{i}{2}\varphi_2 + \frac{\lambda}{2}\varphi_2 - \frac{i}{2}G\left(|\varphi_2|^2\right)\varphi_2 = \frac{i}{2}\varphi_1, \\
&\varphi_1 = \text{const}, \\
&G(z) = \frac{4k}{z}\left(1 - \frac{1}{\sqrt{1+z}}\right).
\end{aligned} \tag{21}$$

Splitting to modulus and argument yields

$$\begin{aligned}
&\varphi_2 = P(\tau_0)\exp(\mathrm{i}\gamma(\tau_0)), \\
&\varphi_1 = C\exp(\mathrm{i}\Gamma).
\end{aligned} \tag{22}$$

Choice of proper initial conditions for Eqs. (21) and (22) is a non-trivial issue. The approximation under consideration is related to time scale $O(1)$, but is not relevant for the very beginning of the transfer process, before the flow approaches the 1:1 resonance manifold. One can suggest that the phases of dynamic variables change very rapidly whereas the average amplitudes remain almost unchanged. Therefore, in order to establish the critical initial amplitude for the TET one can adopt $C = A$, $\Gamma = 0$ (this choice is not significant), $P(0) = A$. The initial phase $\gamma(0)$ cannot be defined in the framework of the averaged equations. For the sake of estimation, we will accept that the TET occurs if for all values of the initial phase $0 < \gamma(0) < \pi$ the averaged flow for time scale $O(1)$ corresponds to excited NES (the sense of the latter statement will be elucidated below). Thus, system (21) is reduced to the form

$$\begin{aligned} &\frac{\partial P}{\partial \tau_0} = -\frac{\lambda}{2}P + \frac{1}{2}A\sin\gamma, \\ &\frac{\partial \gamma}{\partial \tau_0} = -\frac{1}{2} + \frac{2k}{P^2}\left(1 - \frac{1}{\sqrt{1+P^2}}\right) + \frac{A}{2P}\cos\gamma, \\ &P(0) = A, \quad 0 < \gamma(0) < \pi. \end{aligned} \tag{23}$$

It is easy to demonstrate that Eq. (23) can have one or three fixed points, depending on values of k, A and λ. If the fixed point is single it is stable node; pair of saddle and additional node may appear depending on

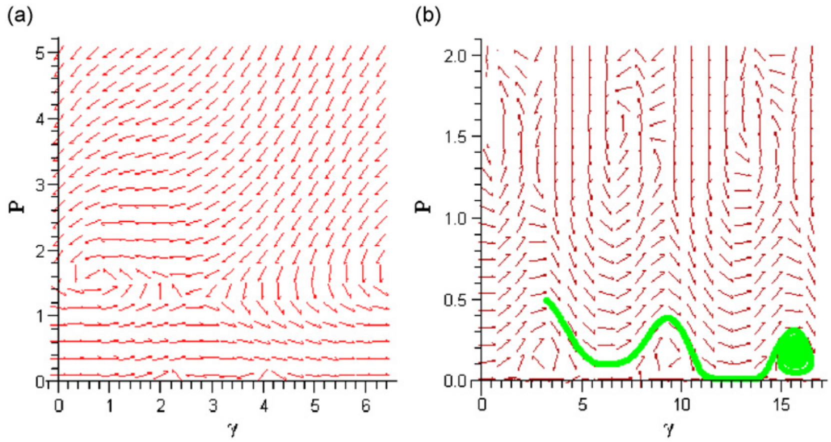

Fig. 5. Phase portrait of system (23), $A = 0.5$: (a) general shape and (b) trajectory with $\gamma(0) = \pi$.

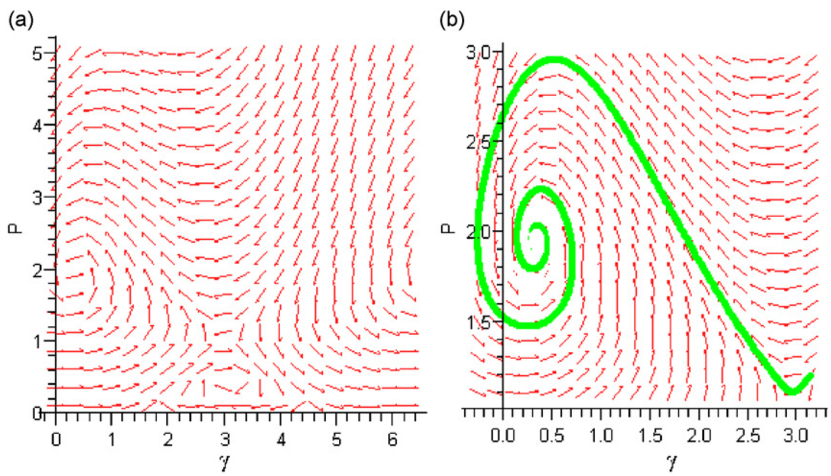

Fig. 6. Phase portrait of system (23), $A = 1.2$: (a) general shape and (b) trajectory with $\gamma(0) = \pi$.

parameters of the system. Typical phase portraits of system (23) and phase trajectories for initial condition $\gamma(0) = \pi$ are presented in Figs. 5 and 6.

For $A > 1.2$ every trajectory with initial phase $0 < \gamma(0) < \pi$ is attracted to the upper fixed point and thus the NES is excited, providing a necessary condition for the TET. Direct numeric simulations of system (18) with initial conditions $y_1(0) = 0, \dot{y}_1(0) = A, y_2(0) = 0, \dot{y}_2(0) = 0$ was performed for $1 < A < 1.5$. The efficient TET was revealed for $A > 1.18$, in satisfactory agreement with the results of the asymptotic analysis presented above.

3.3. Asymptotic analysis—order $O(\varepsilon^{-1})$

For the case of the NES potential (17), approximation (16) for time scale $O(1/\varepsilon)$ is written as

$$\frac{\partial N}{\partial \tau_1} = \frac{-\lambda N}{2\left(1 + \lambda^2 + G^2(N^2) - 2G(N^2) - 2N^2 G'(N^2) + 2N^2 G(N^2) G'(N^2)\right)},$$
$$\frac{\partial \delta}{\partial \tau_1} = \frac{-\lambda^2 + G(N^2) - G^2(N^2) - 2N^2 G(N^2) G'(N^2)}{2\left(1 + \lambda^2 + G^2(N^2) - 2G(N^2) - 2N^2 G'(N^2) + 2N^2 G(N^2) G'(N^2)\right)},$$
$$G(z) = \frac{4k}{z}\left(1 - \frac{1}{\sqrt{1+z}}\right). \tag{24}$$

Qualitative behavior of solutions of system (24) is determined by the structure of the denominator of both equations. Namely, if it does not have zeros and therefore does not change sign (and is positive—it is easy to check it near $N = 0$), then $N(\tau_1)$ decreases monotonously. Still, if the denominator will have zeros, the solutions will become singular. Physically, it means that the flow will be forced to leave the 1:1 resonance manifold. In this case, the energy absorption is greatly enhanced. It is possible to prove that for any value of $k > 0.5$ (which naturally corresponds to possibility of 1:1 resonance capture in the system under consideration) there exists interval of values for the damping coefficient $\lambda \in (0, \lambda_{\max})$ for which the slow flow described by Eq. (24) will exhibit breakdown, leading to efficient dissipation of energy. Value of $\lambda_{\max}$ versus k is presented in Fig. 7.

So, against an intuition, in order to get efficient dissipation one should keep the dissipation coefficient small enough. This point is illustrated in Fig. 8, where the dissipation of energy in system (18) is plotted versus time for $k = 2$ and $A = 1.3$ for two values of damping (below and above the curve in Fig. 7).

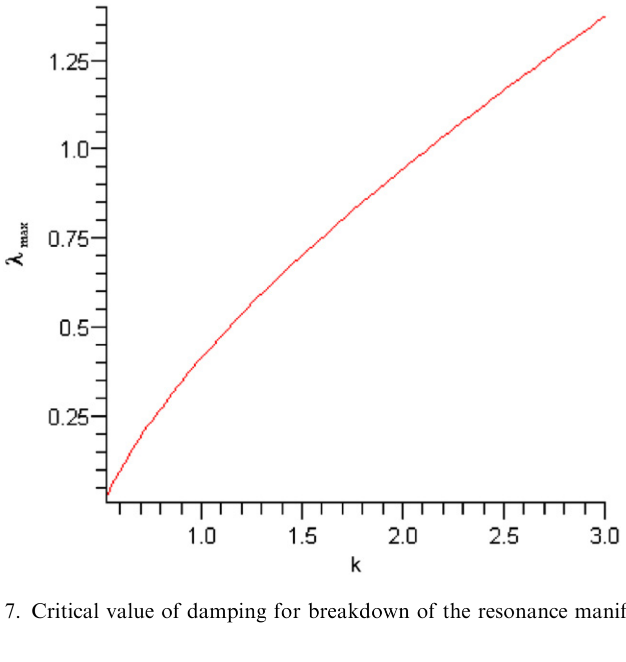

Fig. 7. Critical value of damping for breakdown of the resonance manifold.

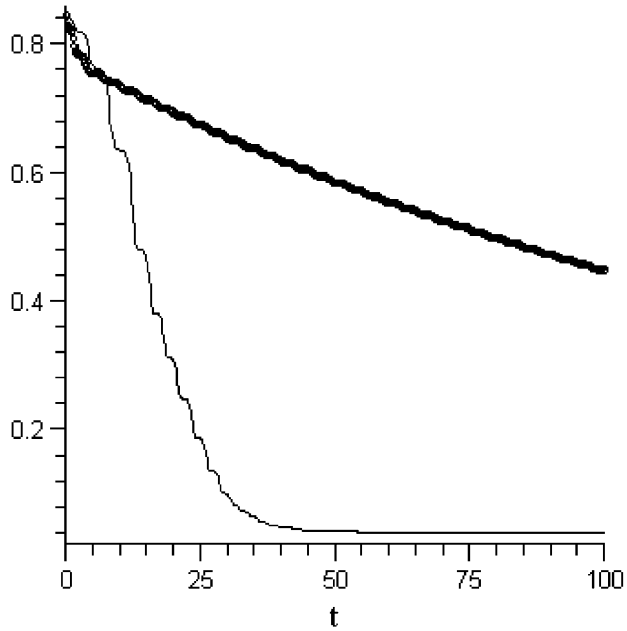

Fig. 8. Energy dissipation for different values of λ (total energy in the system versus time, thick line—$\lambda = 1.2$, thin line—$\lambda = 0.2$).

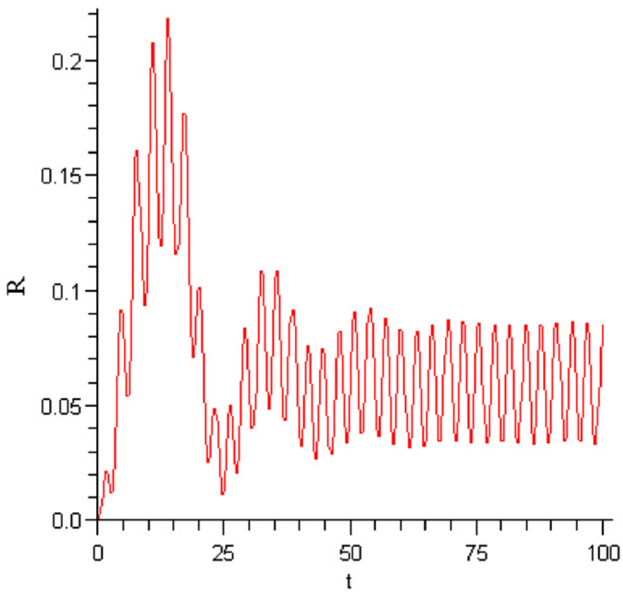

Fig. 9. Relative instantaneous energy in the attachment with piecewise linear potential, $A = 0.6$.

One can conclude that the choice of optimal damping value is crucial for efficient design of the NES.

4. NES with piecewise linear potential

In a recent paper [7], it was demonstrated that the effect of TET may be achieved with the help of NES with a piecewise linear potential. Such design may be preferable since it is comparatively easy in production.

We consider system (1) with force F described by a piecewise linear continuous function:

$$F(z)=\begin{cases}\beta z+(\beta-\alpha)a, & z<-a,\\ \alpha z, & |z|<a,\\ \beta z-(\beta-\alpha)a, & z>a.\end{cases} \tag{25}$$

To illustrate the TET, system (1) with NES force described by Eq. (25) is simulated with initial conditions $y_1(0)=0, \dot{y}_1(0)=A, y_2(0)=0, \dot{y}_2(0)=0$. For the sake of simulation, we choose the values of parameters $a=1,\ \alpha=0.5,\ \beta=2,\ \lambda=0.2,\ \varepsilon=0.05$. Similarly to Section 3, one should study the energy distribution between the primary mass and the NES. The results of this simulation for two different values of A are presented in Figs. 9 and 10.

One can easily recognize characteristic onset of the TET, despite the fact that the "only" nonlinearity in the system is due to the matching of different linear response functions.

The next question is whether the analytic framework developed in Section 2 is suitable for description of the TET in this system with non-analytic potential of the NES. For this sake, the Fourier component of the force should be computed in accordance with Eqs. (8)–(10). Simple but somewhat lengthy calculations yield

$$f_1(\varphi_2,\varphi_2^*)=\begin{cases}-\dfrac{i\alpha}{2}\varphi_2, \quad |\varphi_2|<a\\ -\dfrac{i}{2\pi}\varphi_2\left(\begin{array}{c}\beta\left(2\arccos\dfrac{a}{|\varphi_2|}+\dfrac{2a}{|\varphi_2|}\sqrt{1-\dfrac{a^2}{|\varphi_2|^2}}\right)+\\ +\alpha\left(\pi-2\arccos\dfrac{a}{|\varphi_2|}-\dfrac{2a}{|\varphi_2|}\sqrt{1-\dfrac{a^2}{|\varphi_2|^2}}\right)-\dfrac{4a}{|\varphi_2|}(\beta-\alpha)\sqrt{1-\dfrac{a^2}{|\varphi_2|^2}}\end{array}\right), \quad |\varphi_2|>a.\end{cases} \tag{26}$$

As in Section 3, we check the validity of the averaging procedure for description of the TET by direct comparison between simulated flows of systems (1) with force (25) and (7) combined with (26) with appropriate corresponding initial conditions, computed with the help of anzats (2). We compare the values $Z=\sqrt{\left(y_1(t)-y_2(t)\right)^2+\left(\dot{y}_1(t)-\dot{y}_2(t)\right)^2}$ (solid line) and $Z_{\text{average}}=|\varphi_2|$ (dotted line) (Fig. 11).

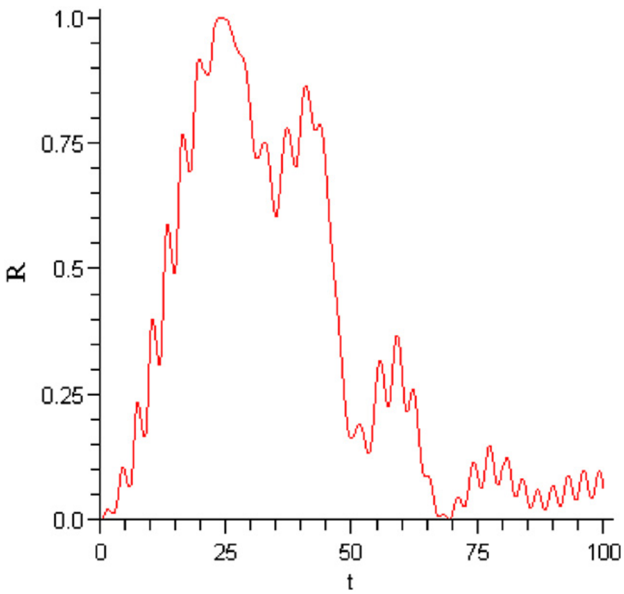

Fig. 10. Relative instantaneous energy in the attachment with piecewise linear potential, $A=0.8$.

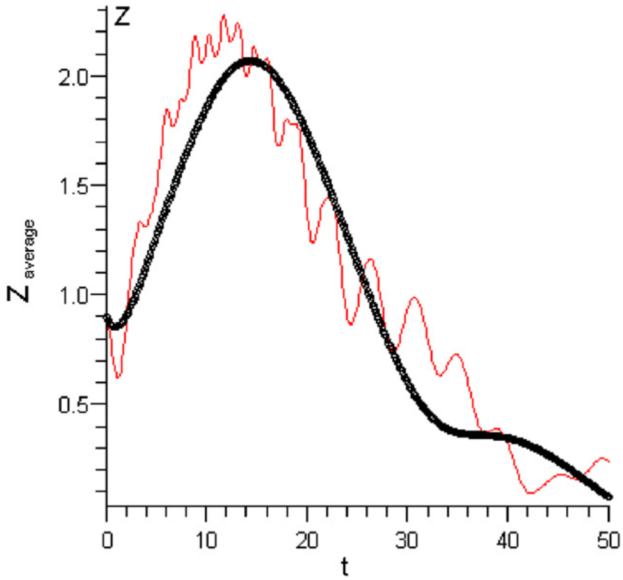

Fig. 11. Comparison between initial flow (solid line) and averaged flow (dotted line) for the system with piecewise linear NES. $A = 0.9$.

Clearly enough, the correspondence is satisfactory and therefore the NES with non-analytic response law (25) may be analyzed with the help of the averaging approach. Function in Eq. (26) has rather complicated shape and therefore it is difficult to handle it analytically. Still, numeric calculation of the roots of Eq. (16) is still straightforward and structure of the solutions is qualitatively the same as in the case of the softening nonlinearity, including finite interval of the damping values where the TET is possible.

5. Concluding remarks

The results presented above allow us to conclude that the NESs with soft or piecewise linear potential may be a rather suitable candidate for dynamical systems involving the TET. Transient responses of these systems with non-polynomial nonlinearities may be successfully treated with the help of Fourier expansion with respect to fast time scale and subsequent averaging. Asymptotic analysis based on small parameter related to the mass ratio yields reliable analytic description of the transfer process and allows optimization of the parameter values.

The method developed in the paper has its obvious restrictions. First of all, the averaging based on the first Fourier component of the nonlinear force term has some chances to yield a reliable description of the process only in the conditions of 1:1 resonance—if other resonances are significant, more components will be involved. Still, the time scale of the problem is limited by damping and one cares only about the first stage of the transient response. There exists a range of initial conditions in which it will be governed by 1:1 resonance [5].

The other complication may arise if the analytic shape of the response forces is not known—for instance, they are obtained from measurements. In this case, the possible approach may be to compute the function $G(z)$ numerically, using Eq. (8). Validity and accuracy of the developed approach in this situation requires additional study.

Acknowledgment

The author is grateful to Israel Science Foundation (Grant 486/05) for financial support.

Appendix A

In this appendix, Bendixson criterion is applied to Eq. (13) and absence of limit cycles is demonstrated. At time scale τ_0, system (13) describes dynamics of variable φ_2 in a two-dimensional state space:

$$\begin{gathered}\frac{\partial\varphi_2}{\partial\tau_0}+\frac{\mathrm{i}}{2}\varphi_2+\frac{\lambda}{2}\varphi_2-\frac{\mathrm{i}\varphi_2}{2}G\left(|\varphi_2|^2\right)=Q,\\ Q=\frac{\mathrm{i}}{2}\varphi_1=\text{const.}\end{gathered}\tag{A.1}$$

By splitting φ_2 to real and imaginary part, one obtains

$$\begin{aligned}&\varphi_2=q_1+\mathrm{i}q_2,\quad q_{1,2}\in\mathbb{R},\\ &\frac{\partial q_1}{\partial\tau_0}=\frac{1}{2}q_2-\frac{\lambda}{2}q_1-\frac{q_2}{2}G\left(q_1^2+q_2^2\right)+\mathrm{Re}(Q)=h_1(q_1,q_2),\\ &\frac{\partial q_2}{\partial\tau_0}=-\frac{1}{2}q_1-\frac{\lambda}{2}q_2+\frac{q_1}{2}G\left(q_1^2+q_2^2\right)+\mathrm{Im}(Q)=h_2(q_1,q_2).\end{aligned}\tag{A.2}$$

Divergence of the vector field on plane (q_1, q_2) determined by Eq. (A.2), is expressed as

$$\operatorname{div}\vec{h}=\frac{\partial h_1}{\partial q_1}+\frac{\partial h_2}{\partial q_2}=-\lambda<0.\tag{A.3}$$

So, the divergence of the vector field is always negative; therefore, in accordance with the Bendixson criterion, the limit cycles are absent.

Appendix B

Let us compute the expression for function $G(z)$ for the response force of the attachment described by potential (17)

$$F(w)=V'(w)=\frac{2kw}{1+w^2},\tag{B.1}$$

$$\begin{aligned}f_1&=\frac{1}{2\pi}\int_0^{2\pi}F\left(-\frac{\mathrm{i}}{2}\left(\varphi_2\exp(\mathrm{i}t)-\varphi_2^*\exp(-\mathrm{i}t)\right)\right)\exp(-\mathrm{i}t)\,\mathrm{d}t\\ &=\frac{k}{\pi}\int_0^{2\pi}\frac{-\mathrm{i}/2\left(\varphi_2\exp(\mathrm{i}t)-\varphi_2^*\exp(-\mathrm{i}t)\right)}{1+\left(-\mathrm{i}/2\left(\varphi_2\exp(\mathrm{i}t)-\varphi_2^*\exp(-\mathrm{i}t)\right)\right)^2}\exp(-\mathrm{i}t)\,\mathrm{d}t.\end{aligned}\tag{B.2}$$

By splitting into modulus and argument parts $\varphi_2=C\exp(\mathrm{i}\gamma)$, one obtains

$$-\frac{\mathrm{i}}{2}\left(\varphi_2\exp(\mathrm{i}t)-\varphi_2^*\exp(-\mathrm{i}t)\right)=-\frac{\mathrm{i}C}{2}(\exp(\mathrm{i}(t+\gamma))-\exp(-\mathrm{i}(t+\gamma))=C\sin(t+\gamma).\tag{B.3}$$

Substitution of (B.3)–(B.2) yields

$$\begin{aligned}f_1&=\frac{k}{\pi}\int_0^{2\pi}\frac{C\sin(t+\gamma)}{1+C^2\sin^2(t+\gamma)}\exp(-\mathrm{i}t)\,\mathrm{d}t=\frac{k\exp(\mathrm{i}\gamma)}{\pi}\int_0^{2\pi}\frac{C\sin(t+\gamma)}{1+C^2\sin^2(t+\gamma)}(\cos(t+\gamma)-\mathrm{i}\sin(t+\gamma))\,\mathrm{d}t\\ &=\frac{k\exp(\mathrm{i}\gamma)}{\pi}(I_1-\mathrm{i}I_2)\\ I_1&=\int_0^{2\pi}\frac{C\sin(t+\gamma)\cos(t+\gamma)}{1+C^2\sin^2(t+\gamma)}\,\mathrm{d}t=0\\ I_2&=\int_0^{2\pi}\frac{C\sin^2(t+\gamma)}{1+C^2\sin^2(t+\gamma)}\,\mathrm{d}t=\frac{1}{C}\int_0^{2\pi}\left(1-\frac{1}{1+C^2\sin^2(t+\gamma)}\right)\mathrm{d}t=\frac{2\pi}{C}\left(1-\frac{1}{\sqrt{1+C^2}}\right).\end{aligned}\tag{B.4}$$

Finally, combining all above results, one obtains

$$f_1 = -\frac{i\varphi_2}{2}\frac{4k}{|\varphi_2|^2}\left(1 - \frac{1}{\sqrt{1+|\varphi_2|^2}}\right). \tag{B.5}$$

Comparing this expression with Eq. (10), one obtains the shape of $G(z)$ in Eq. (20).

References

[1] O.V. Gendelman, Transition of energy to nonlinear localized mode in highly asymmetric system of nonlinear oscillators, *Nonlinear Dynamics* 25 (2001) 237–253.

[2] A.F. Vakakis, O.V. Gendelman, Energy pumping in nonlinear mechanical oscillators II: resonance capture, *Journal of Applied Mechanics* 68 (2001) 42–48.

[3] O.V. Gendelman, Bifurcations of nonlinear normal modes of linear oscillator with strongly nonlinear damped attachment, *Nonlinear Dynamics* 37 (2004) 115–128.

[4] Y.S. Lee, G. Kerschen, A.F. Vakakis, P.N. Panagopoulos, L.A. Bergman, D.M. McFarland, Complicated dynamics of a linear oscillator with an essentially nonlinear local attachment, *Physica D* 204 (2006) 41–69.

[5] P.N. Panagopoulos, O. Gendelman, A.F. Vakakis, Robustness of nonlinear targeted energy transfer in coupled oscillators to changes of initial conditions, *Nonlinear Dynamics* 47 (2007) 377–387.

[6] E. Gourdon, C.H. Lamarque, Nonlinear energy sinks with uncertain parameters, *Journal of Computational and Nonlinear Dynamics* 1 (2006) 187–195.

[7] F. Georgiadis, A.F. Vakakis, D.M. McFarland, L.A. Bergman, Shock isolation through passive energy pumping I a system with piecewise linear stiffnesses, *CD-ROM Proceedings of ASME 2003 Design Engineering Technical Conferences and Computers and Information in Engineering Conference*, Chicago, IL, USA, September 2–6, 2003, Paper VIB-48490.

[8] L.I. Manevitch, The description of localized normal modes in a chain of nonlinear coupled oscillators using complex variables, *Nonlinear Dynamics* 25 (2001) 95–109.

[9] O.V. Gendelman, L.I. Manevitch, Method of complex amplitudes: harmonically excited oscillator with strong cubic nonlinearity, *CD-ROM Proceedings of DETC.03 ASME 2003 Design Engineering Technical Conferences and Computers and Information in Engineering Conference*, Chicago, IL, USA, September 2–6, 2003, Paper VIB-48586.